Acta Crystallographica Section A
Foundations of Crystallography
ISSN 0108-7673

Received 10 December 2010
Accepted 12 March 2011

Faulting in finite face-centered-cubic crystallites

Kenneth R. Beyerlein,[a,b]* Robert L. Snyder[a] and Paolo Scardi[b]

[a]Materials Science and Engineering, Georgia Institute of Technology, 771 Ferst Drive, Atlanta, GA 30332, USA, and [b]Department of Materials and Industrial Technology, University of Trento, via Messiano 77, I-38123 Trento, Italy. Correspondence e-mail: ken.beyerlein@mse.gatech.edu

The effects that planar faults have on the powder diffraction peak profiles of a face-centered cubic (f.c.c.) material are studied considering the case of small crystallites. In doing so a new method to calculate the planar probability correlation function of a faulted crystallite is presented which considers the finite extent of the planar sequence. The resulting correlation function is demonstrated to be dependent on the position of a fault in a crystallite through its proximity to a crystallite boundary. The average correlation function found considering equal probability of a fault existing on each plane in a crystallite is compared with that found by solving a system of recursion relations. The broadened subcomponents of the f.c.c. powder profiles are shown to be related to the correlation function through a general Fourier series expression. This expression is then used to simulate peak profiles from the developed model, and then compare them with those predicted by the recursion relation treatment.

1. Introduction

The study of a diffraction spot, or profile, to extract information on the stacking faults contained in the material dates back to the 1930s (Hendricks *et al.*, 1930). Since this early work on cobalt, the theoretical description of how faulting influences the diffraction pattern has been repeatedly refined, extending it to low-symmetry crystal structures and complex faulting configurations (Estevez-Rams *et al.*, 2007). However, it has not been widely considered how the effect of faulting changes as the crystallite becomes small, or when the fault is positioned near a crystallite boundary. These considerations become increasingly important to characterize the nanomaterials which are being developed for use in modern technologies. We will limit our discussion to the well established case of faulting in face-centered cubic (f.c.c.) domains, to serve as an example of how a small crystallite size influences the features observed in the powder pattern from faulting.

Beginning with the description of Warren (1990), the intensity in reciprocal space from a finite crystallite containing faults can be expressed as

$$I = \psi^2 \sum_{m=-\infty}^{\infty} N_m \langle \exp(i\phi(m)) \rangle \exp(2\pi i m h_3/3). \quad (1)$$

In this expression (Warren, 1990, equation 13.39) the f.c.c. lattice is described in terms of a hexagonal lattice with continuous reciprocal-space coefficients h_1 and h_2 defined in the (111) plane and h_3 normal to the plane. The symbol ψ^2 represents the form factor of the planes and is factorized outside the sum by approximating the crystallite as a columnar stack of (111) planes with equivalent cross sections. The term N_m represents the number of pairs of planes separated by a distance md_{111}, where m is an integer and d_{111} is the distance between planes in the stack, and $\langle \exp(i\phi(m)) \rangle$ is the average phase factor due to the relative displacement of each plane. This factor is determined considering how the phase changes when scattering occurs from two planes of different type. Since f.c.c. can be represented as an ABC stacking, there are only three distinct phase factors:

$\phi_0(m) = 0$ when the pair is of the same type (*i.e.* AA);

$\phi_1(m) = -2\pi(h_1 - h_2)/3$ when the pair is a positive sequence (*i.e.* AB); and

$\phi_2(m) = 2\pi(h_1 - h_2)/3$ when the pair is a negative sequence (*i.e.* AC).

The average phase factor is then expressed as

$$\langle \exp(i\phi(m)) \rangle = P_0(m) \exp(i\phi_0(m)) + P_1(m) \exp(i\phi_1(m)) + P_2(m) \exp(i\phi_2(m)), \quad (2)$$

where $P_i(m)$ is the probability of finding a pair of planes of the type i, separated by m planes. In a powder, symmetry exists between $P_1(m)$ and $P_2(m)$ because a positive stacking sequence will then become negative when observed from the opposite point of view. Therefore, these two probabilities are equal and utilizing the normalization condition gives

$$\langle \exp(i\phi(m)) \rangle = P_0(m) + (1 - P_0(m)) \cos(2\pi(h_1 - h_2)/3). \quad (3)$$

Therefore, the effect of faulting on the powder pattern of f.c.c. crystallites is completely determined by the probability correlation function, $P_0(m)$.

Most existing methods to calculate this function rely on a probabilistic treatment, similar to the initial works of Hendricks & Teller (1942), as well as Wilson (1942), which relate the probability of a fault existing on a given plane to the

type of the preceding plane. A parametrized form of a modulating function is then assumed and recursion relations are used to solve the correct parameters (Warren, 1990; Estevez-Rams *et al.*, 2008). The appeal of this recursion approach is that it allows for the direct determination of the fault probability in the sample independent of crystallite size. However, the assumptions made in solving the equations are not suited for small crystallites. First, many of the developed recursion solutions assume intrinsically an infinitely large stack, which does not consider how a surface might influence the planar correlation. One proposed general solution for a finite stack is based on a self-similar recursion treatment, and was developed by Treacy (Treacy *et al.*, 1991) for use in the diffraction pattern simulation software *DIFFaX*. However, it relies on a statistical description of the interplanar transitions which are the same throughout the crystallite and for a crystallite of any size. Therefore, the effect of a surface on these transition probabilities has not been handled explicitly. Further assumptions which are not suitable for small crystallites are: a sequence consisting of only a few layers is considered to set up the recursion equations, and each layer is given an equal probability of containing a fault plane. This does not allow for possible control over the position of the fault in a crystallite, and in fact assumes that any arrangement of multiple faults is equally probable conserving the global fault probability. An alternative to this description was first developed by Jagodzinski, who considered more layers in the recursion relations (Jagodzinski, 1949*a*,*b*). However, in this case the infinite stack assumption was again used in solving the final form of the correlation function.

In order to study the effect of faulting in a small crystallite it is necessary to develop a different strategy to calculate the probability correlation function. In our approach, first a basic understanding of how a fault changes the correlation between a pair of planes is discussed. Then it will be shown how a termination in the sequence affects this correlation, and simple statistical reasoning will be used to derive analytical expressions for the probability correlation function of a finite stack containing a fault. Finally, an ensemble average of these expressions is carried out to obtain a form of probability correlation function more consistent with that observed in a powder. A demonstration of the resulting diffraction profiles concludes this study along with a comparison with peak profiles obtained assuming the latest formulation of the recursion method solution for f.c.c. materials. This type of model is especially suited for small crystalline domains, thin films or metal nanoparticles, whose energetics do not allow for large numbers of faults within a given domain. It is then not suited to study multiple twinned particles, which can contain three or five twin faults arranged in a non-crystallographic symmetry (Marks, 1994; Cervellino *et al.*, 2003).

2. Effect of deformation faults

To understand how faulting changes the correlation between planes, it is enough to study an example stacking sequence before and after the creation of a fault. Here we will only consider the forward stacking direction and later account for the opposite stacking direction in the calculation of the powder diffraction pattern [see discussion leading to equation (3)]. The f.c.c. lattice is represented as a stack of (111) planes and the *ABC* convention is used to denote the three different plane types. As shown in the following examples the fault position is denoted by a pipe '|' in the sequence.

$$\ldots ABCABCA \ldots \text{ (perfect)} \tag{4a}$$

$$\ldots ABCA|CAB \ldots \text{ (deformation fault)} \tag{4b}$$

$$\ldots ABCA|CBA \ldots \text{ (twin fault)} \tag{4c}$$

Any pair of planes can be characterized by the number of planes which are spanned, m, and the number of steps between these planes in a forward permutation, which we will call the pair type, i [*i.e.* $i = 1$ for (AB) and $i = 2$ for (AC)]. It is readily noticed that for a perfect stacking sequence all pairs with a separation m are of type i, where $i \equiv m \bmod n$ and n is the number of different plane types in the sequence. A separation, m, can then be said to belong to the set m_i, making the calculation of $P_0(m)$ trivial for an infinite perfect stacking sequence. In this case all spacings in the set m_0 are between pairs of type 0, implying $P_0(m_0) = 1$, and these are the only spacings between pairs of type 0, so $P_0(m_{i\neq 0}) = 0$.

By studying the planar sequence of equation (4*b*) we find that a deformation fault affects the planes after the fault by changing them to the next type in the forward permutation sequence. Also, only a pair of planes which has a fault between them will have their pair type affected by this change. Comparison of stacking sequences with and without a deformation fault, such as those depicted in equations (4*a*) and (4*b*), finds that a pair, Δ_i, which spans a fault will change its type, i, following

$$\Delta_0 \overset{\text{f}}{\rightarrow} \Delta_1', \quad \Delta_1 \overset{\text{f}}{\rightarrow} \Delta_2' \quad \text{and} \quad \Delta_2 \overset{\text{f}}{\rightarrow} \Delta_0'. \tag{5}$$

In these relations the pairs which do not span a fault are depicted on the left of the arrow, while on the right denoted with an apostrophe are the new pair types due to the pair spanning a fault. By this notation, the transformation of $(AA) \overset{\text{f}}{\rightarrow} (AB)'$ falls in the case of $\Delta_0 \overset{\text{f}}{\rightarrow} \Delta_1'$. A stacking fault then not only increments the plane type, but also has the effect of incrementing the pair type.

In an infinite stack the number of pairs separated by m planes which can span a fault is always m. However, in a finite stack the number of pairs which span a fault depends on the distance from the fault plane to a surface boundary. For example, considering the finite stacks

$$ABCA|CABCABC \ (p = 4)$$
$$ABC|BCABCABC \ (p = 3)$$
$$AB|ABCABCABC \ (p = 2),$$

it is evident that in the case of the first fault position depicted, $p = 4$, four distinct pairs having a spacing of four planes ($m = 4$) can span the fault plane. When the fault position is moved to $p = 3$, only three such pairs span the fault and similarly two

pairs for $p = 2$. Considering other pair separations it is found that the number of pairs which span a fault, N_f, is dependent on both the spacing, m, and the fault position, p, and is conditionally expressible as

$$N_f(N, m, p') = \begin{cases} m & m \le p' \\ p' & p' < m \le N - p' \\ N - m & N - p' < m. \end{cases} \quad (6)$$

Here p' is the number of planes from the fault to the *nearest* surface, and for a deformation fault

$$p' = \begin{cases} p & p \le N/2 \\ N - p & N/2 < p. \end{cases}$$

The case of $N - p' < m$ in equation (6) means both boundaries are limiting the number of pairs which span the fault, and all pairs in the stack of separation m span the fault.

Using this relationship and the relations of equation (5), the probability correlation function for a finite stack containing a deformation fault can be derived. If $m \in m_0$ every pair which spans the fault will become a 1-type, so the fraction of pairs which are 0-type is the complement of the fraction which spans the fault. When $m \in m_1$, the number of pairs which become 0-type does not change, and when $m \in m_2$ the fraction of faults which become 0-type is the fraction which spans the fault. These observations, along with equation (6), result in a probability correlation function of the form

$$P_0(m) = \begin{cases} \dfrac{m_0}{1 - \dfrac{m}{N-m}}, & \dfrac{m_1}{0,} & \dfrac{m_2}{\dfrac{m}{N-m}} & m \le p' \\ \dfrac{}{1 - \dfrac{p'}{N-m}}, & \dfrac{}{0,} & \dfrac{}{\dfrac{p'}{N-m}} & p' < m \le N - p' \\ 0, & 0, & 1 & N - p' < m. \end{cases} \quad (7)$$

A series of correlation functions calculated using this relationship is shown in Fig. 1 for a 50-layer stack containing a deformation fault at different positions. When the fault is near the boundary the planar correlation resembles that of a perfect f.c.c. stack as only correlations for large m are altered. As the fault is moved toward the center of the stack the $P_0(m)$ for smaller separations become increasingly affected. After the fault crosses the middle of the stack a symmetry is observed for the cases of $p = 15$ and $p = 35$, as well as $p = 5$ and $p = 45$, due to their equivalent distance to the nearest surface, p'.

3. Effect of twin faults

The same general treatment described in the previous section can be adopted to study the case of a finite stacking sequence containing a twin fault. Considering a twin located on an A plane, as in the stack shown in equation (4*c*), we find that the twin fault has the following effects on pair type:

$$\begin{aligned} &(AA) \xrightarrow{t} (AA)', \quad (BB) \xrightarrow{t} (BC)', \quad (CC) \xrightarrow{t} (CB)', \\ &(AB) \xrightarrow{t} (AC)', \quad (BC) \xrightarrow{t} (BB)', \quad (CA) \xrightarrow{t} (CA)', \\ &(AC) \xrightarrow{t} (AB)', \quad (BA) \xrightarrow{t} (BA)', \quad (CB) \xrightarrow{t} (CC)', \end{aligned} \quad (8)$$

where now the t above the arrow signifies that transformations are due to the pair spanning a twin fault. Unlike the case of the deformation fault, the expressions in equation (8) are now specifically dependent on the pair and twin plane, so the Δ_i notation has not been used. Here we only describe the case of a twin on an A-type plane, but analogous expressions are found for a twin on a B or C plane. The transformations like those in equation (8) define the important pairs to consider when calculating $P_0(m)$. For instance, for the case of an A-type twin it becomes apparent that $P_0(m_0)$ of an ideal stacking will be decreased by an amount proportional to the number of (BB) and (CC) pairs which span the twin fault. Also, $P_0(m_1)$ will be increased by an amount related to the number of (BC) pairs spanning the fault, and similarly $P_0(m_2)$ will be increased by the proportion of (CB) pairs. Assuming the fault is not near a boundary, we find that the number of important pairs has a solution independent of the fault type:

$$N_0(m, m \le p) = \begin{cases} 2m/3 & m \in m_0 \\ (m-1)/3 & m \in m_1 \\ (m+1)/3 & m \in m_2, \end{cases} \quad (9)$$

where N_0 is the number of pairs which span the twin fault and influence $P_0(m)$ – the second criterion being what differentiates this quantity from N_f, defined in equation (6).

When the number of important pairs becomes influenced by the presence of a surface boundary, the relationship describing their abundance becomes dependent on the twin plane type. We will define the twin plane type, t, relative to its distance from the *left* boundary by $t \equiv p \bmod n$. The number of important pairs for $p' < m \le N - p'$ is found by considering a sequence without a boundary, and subtracting the number which are missing due to the nearest boundary. This can be expressed as

$$N_0(p') = N_0(m, m \le p') - N_X^{m-p'}, \quad (10)$$

where $N_X^{m-p'}$ is the number of planes of type X in a perfect stack of length $(m - p')$. The plane type, X, is determined as the first plane of an important pair for a given twin type. For instance, considering again an A-type twin ($t = 1$), when $m \in m_1$, the important pair is (BC), so X is B in this case. Using expression (10), and considering the three possible twin types, the following expression for N_0 when $p' < m \le N - p'$ is found:

$$N_0(m, p' < m \le N - p') = \begin{cases} (2p' + a_0)/3 & m \in m_0 \\ (p' + a_1)/3 & m \in m_1 \\ (p' + a_2)/3 & m \in m_2, \end{cases} \quad (11)$$

where the constants, a_i, have a dependence on the twin type, t, and are given in Table 1.

The final case to consider is when the planar spacing is large enough that the correlation function is influenced by both surfaces. Now all pairs in the system span the fault so it is

Table 1
Constants for $N_0(m)$ of equation (11).

	a_0	a_1	a_2
$t=0$	0	0	0
$t=1$	−2	−1	−1
$t=2$	−1	−2	1

Table 2
Constants for $N_0(m)$ of equation (12).

	b_0			b_1			b_2		
	$s=0$	$s=1$	$s=2$	$s=0$	$s=1$	$s=2$	$s=0$	$s=1$	$s=2$
$t=0$	0	1	2	1	0	2	−1	1	0
$t=1$	0	−2	−1	1	0	−1	−1	−2	0
$t=2$	0	1	−1	−2	0	−1	2	1	0

necessary to determine the number of important pairs which exist in a stack of length N. In doing so one finds $N_0(m)$ is not only a function of the fault type, which determines the important pairs, but also is dependent on the extent of the stacking. Therefore, we can define the stack type, s, as, $s \equiv N \bmod n$. Again, considering all possible combinations of s, t and m it is found that $N_0(N-m)$ takes the form

$$N_0(m, N-p'<m) = \begin{cases} (2(N-m)+b_0)/3 & m \in m_0 \\ ((N-m)+b_1)/3 & m \in m_1 \\ ((N-m)+b_2)/3 & m \in m_2, \end{cases} \quad (12)$$

where the constants, b_i, are given in Table 2 for the possible combinations of t and s.

Putting together the three discussed cases, the probability correlation function for a finite stack of N planes containing a twin fault at position p is given by

$$P_0(m) = \begin{cases} \underline{m_0} & \underline{m_1} & \underline{m_2} & \\ 1-\dfrac{2m}{3(N-m)}, & \dfrac{m-1}{3(N-m)}, & \dfrac{m+1}{N-m} & m \le p' \\ 1-\dfrac{2p'+a_0}{3(N-m)}, & \dfrac{p'+a_1}{3(N-m)}, & \dfrac{p'+a_2}{3(N-m)} & p' < m \le N-p' \\ 1-\dfrac{2(N-m)+b_0}{3(N-m)}, & \dfrac{(N-m)+b_1}{3(N-m)}, & \dfrac{(N-m)+b_2}{3(N-m)} & N-p' < m. \end{cases} \quad (13)$$

It should be noted that, just like for deformation faults, p' is actually the distance of the twin plane to the nearest boundary. However, for twins the fault position changes depending on which boundary is considered. For example, a twin position defined from the left boundary is *ABCAB*|*ACBA*, as the disruption in the stacking is only evident *after* the fifth plane. However, the twin position for the same stack starting from the right boundary and moving to the left is *ABCA*|*BACBA*. Therefore, it follows for twins

$$p' = \begin{cases} p & p \le (N+1)/2 \\ N-p+1 & (N+1)/2 < p. \end{cases}$$

This relationship also defines the symmetry of $P_0(m)$ with respect to the twin position (*i.e.* the case of $p = 5$ is equivalent to $p = N-4$).

The probability correlation functions given by equation (13) for a planar stack containing a twin at different positions are plotted in Fig. 2. The effect of a twin fault on the planar correlation is seen to be strikingly different to that of a

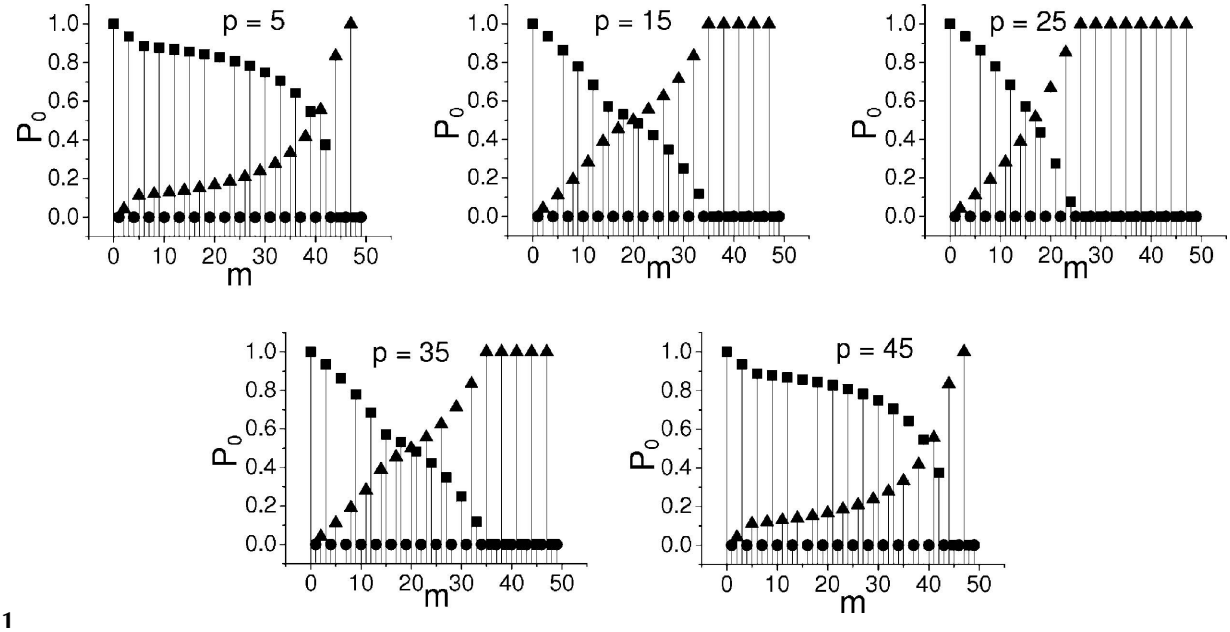

Figure 1
The probability correlation functions, $P_0(m)$, calculated using equation (7) are depicted for a 50-layer stack containing a deformation fault at a series of positions, p. In each case the values of the set m_0 are denoted by squares, those of the set m_1 by circles, and those of the set m_2 by triangles to allow for their clear distinction.

deformation fault, depicted in Fig. 1, as the function now tends to 1/3 for large m, and the values for the set m_1 are no longer zero. It is apparent that as the twin moves beyond the center of the stack, positions like $p = 5$ and $p = 45$ result in similar correlation functions, but differ at larger m, as the rule for twin position symmetry is not exactly observed in this case.

4. Average fault position

The above expressions can be used to derive the average probability correlation function that results from a system of crystallites each containing one fault at different positions. This quantity is of more interest to powder diffraction since the observed pattern is the result of an averaging over the intensity from many crystallites in a sample. For the moment, assuming that all crystallites in a system contain the same number of planes, the average correlation function is given simply as

$$\overline{P_0(m)} = \sum_p w_p P_0(m), \tag{14}$$

where w_p is the number fraction of the fault positions considered in the average and thus must follow $\sum_p w_p = 1$. Neglecting any consideration of fault energetics, the most straightforward assumption is one where all fault positions are equally probable. While possibly unjustified in some cases, this assumption puts the developed model on similar footing as previous models for the effect of faulting on the diffracted intensity, as it is commonly assumed that all planes have an equal probability of containing a fault. In this case for crystallites containing a deformation fault the sum over p in equation (14) is from the first plane to the $N-1$ plane, because a deformation fault on the Nth plane does not result in a fault in the stacking sequence. The number fraction for an equally probable fault position is then given by $w_p = 1/(N-1)$. The expression for the correlation function of this average fault position can be solved analytically by considering two cases, that of $0 \le m < N/2$ and $N/2 \le m \le (N-1)$. For the first case the average probability correlation function when $m \in m_0$ is given by

$$\overline{P_0(m)} = \frac{2\sum_{p'=1}^{m}[1 - p'/(N-m)] + 2\sum_{p'=m+1}^{N/2}[1 - m/(N-m)]}{N-1}$$

$$\overline{P_0(m)} = 1 - \frac{m}{N-1},$$

while in the second case for $N/2 < m \le N-1$, the average probability correlation function is expressed as

$$\overline{P_0(m)} = \frac{2\sum_{p'=1}^{N-m-1}[1 - p'/(N-m)] + 2\sum_{p'=N-m}^{N/2} 0}{N-1},$$

$$\overline{P_0(m)} = 1 - \frac{m}{N-1}.$$

In the above derivation only the relations for the set of m_0 were shown, but following the same steps expressions for m_1 and m_2 can be derived. The final expression for the average correlation function for a system of crystallites each containing one deformation fault is then found to be

$$\overline{P_0(m)} = \begin{cases} m_0 & m_1 & m_2 \\ 1 - \dfrac{m}{N-1}, & 0, & \dfrac{m}{N-1}. \end{cases} \tag{15}$$

The average fault position correlation function for crystallites containing a twin fault is also calculated in this way. However, in this case only $N-2$ twin positions are considered, since the twin positions $p = 1$ and $p = N$ result in a planar correlation which is the same as a perfect stack. Following the steps as for the deformation fault case, and properly accounting for the a_i

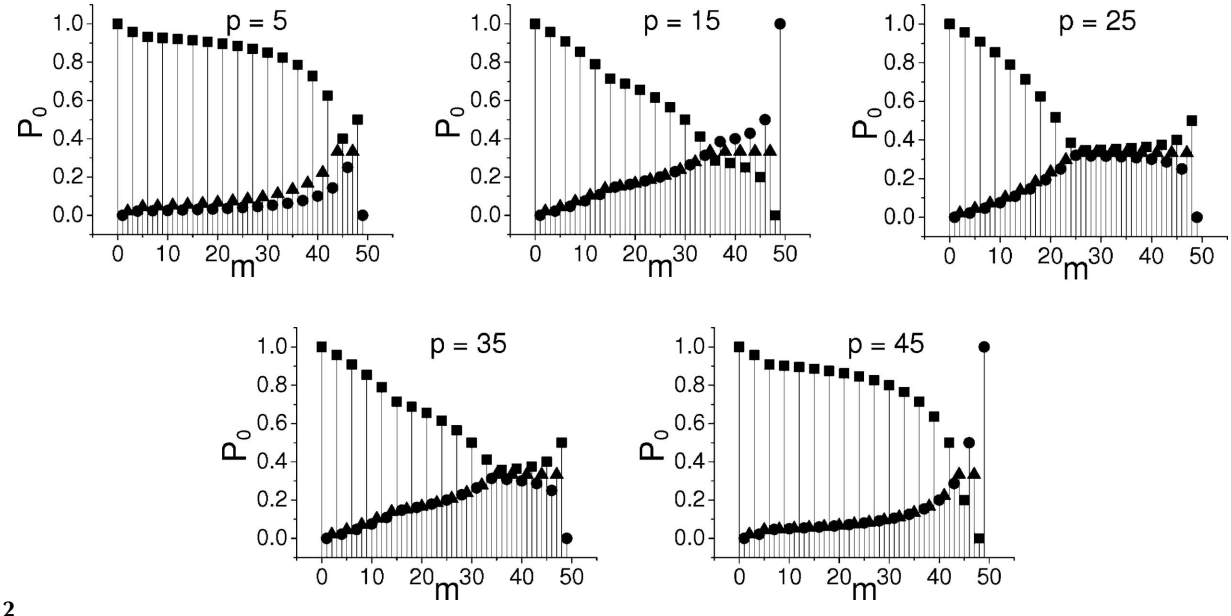

Figure 2
The series of $P_0(m)$ shown has been calculated using equation (13) for a stack containing a twin fault at different positions, p. The sets m_i are denoted by the same shapes as in Fig. 1.

and b_i constants, results in an average correlation function of the form

$$\overline{P_0(m)} = \begin{cases} \underline{m_0} & \underline{m_1} & \underline{m_2} \\ 1 - \dfrac{2m}{3(N-2)}, & \dfrac{m-1}{N-2}, & \dfrac{m+1}{N-2}. \end{cases} \quad (16)$$

It is then interesting to compare this form of the correlation function with that derived from the recursion equation method. The expression for the probability correlation function given by Estevez-Rams (E-R; Estevez-Rams *et al.*, 2008) is the most recent form which has been derived for faulting in close-packed f.c.c. lattices. The average correlation function for a powder of crystallites of 50 layers containing one fault is compared to the E-R correlation function for a stacking sequence of the same fault probability ($\alpha = 1/50$ or $\beta = 1/50$) in Fig. 3. The difference between these expressions, shown below the correlation functions, clearly depicts how these models deviate with increasing correlation length. The E-R model decays slower than the derived model, and asymptotically tends to the value of 1/3 for both deformation and twin faults. Differences in the trends are expected because, as previously discussed, the recursion relation method is solved assuming an infinite stack and intrinsically allows for the possibility that a crystallite contains multiple faults in terms of increasing faulting probability. The developed models, instead, are more specific and only consider the effect of one fault in a finite stack of layers.

5. Limit of $P_0(m)$ as N becomes large

The fault position and pair spacing can be expressed in terms of the stack length N,

$$m = \mu N \quad 0 \le \mu < 1$$
$$p = \rho N \quad 0 < \rho < 1,$$

where μ and ρ are fractional coefficients. Substituting these expressions into equation (7), the probability correlation function for a stack containing a deformation fault then becomes independent of N,

$$P_0(m) = \begin{cases} \underline{m_0} & \underline{m_1} & \underline{m_2} & \\ 1 - \dfrac{\mu}{1-\mu}, & 0, & \dfrac{\mu}{1-\mu} & \mu \le \rho \\ 1 - \dfrac{\rho}{1-\mu}, & 0, & \dfrac{\rho}{1-\mu} & \rho < \mu \le 1-\rho \\ 0, & 0, & 1 & 1-\rho < \mu. \end{cases} \quad (17)$$

This independence of N means that the effect of a single deformation fault on the correlation function is the same regardless of the domain size.

The case of a twin fault is different. Substituting the new expressions for m and p into equation (13), a functional dependence on N remains from equations (11) and (12), and the expression of $P_0(m)$ for a twin becomes

$$P_0(m) = \begin{cases} \underline{m_0} & \underline{m_1} & \underline{m_2} & \\ 1 - \dfrac{2\mu}{3(1-\mu)}, & \dfrac{\mu}{3(1-\mu)}, & \dfrac{\mu}{3(1-\mu)} & \mu \le \rho \\ 1 - \dfrac{2\rho + a_0/N}{3(1-\mu)}, & \dfrac{\rho + a_1/N}{3(1-\mu)}, & \dfrac{\rho + a_2/N}{3(1-\mu)} & \rho < \mu \le 1-\rho \\ 1 - \dfrac{2(1-\mu) + b_0/N}{3(1-\mu)}, & \dfrac{(1-\mu) + b_1/N}{3(1-\mu)}, & \dfrac{(1-\mu) + b_2/N}{3(1-\mu)} & 1-\rho < \mu. \end{cases} \quad (18)$$

Therefore, some terms in the planar correlation function of a twinned stack have a $1/N$ dependence, which will be prevalent for *small* domain sizes. As N becomes large the constants a_i/N and b_i/N go to zero and this expression can be approximated as

$$P_0(m) = \begin{cases} \underline{m_0} & \underline{m_1} & \underline{m_2} & \\ 1 - \dfrac{2\mu}{3(1-\mu)}, & \dfrac{\mu}{3(1-\mu)}, & \dfrac{\mu}{3(1-\mu)} & \mu \le \rho \\ 1 - \dfrac{2\rho}{3(1-\mu)}, & \dfrac{\rho}{3(1-\mu)}, & \dfrac{\rho}{3(1-\mu)} & \rho < \mu \le 1-\rho \\ \frac{1}{3}, & \frac{1}{3}, & \frac{1}{3} & 1-\rho < \mu. \end{cases} \quad (19)$$

The error introduced when using the large N expression is $1/N$, so a stack of 100 layers containing a twin fault will be within roughly 1% of the exact expression when using equation (19) rather than equation (13). This size dependence is not possible to observe in the correlation functions derived from recursion relations due to the previously discussed infinite stack assumption.

6. Calculation of powder diffraction peak

The remainder of this study will be focused on the powder diffraction peak profile resulting from the described models for the planar correlation function. As discussed by Warren (1990), the average phase factor for a powder in equation (3) can take on two forms,

$$\langle \exp(i\phi(m)) \rangle = \begin{cases} 1 & L_0 = 0 \pmod 3 \\ (3P_0(m) - 1)/2 & L_0 = \pm 1 \pmod 3, \end{cases}$$

where L_0 is related to the f.c.c. peak indices by $L_0 = h + k + l$. Since the average phase factor is not affected by a change in the probability correlation function, when $L_0 = 0 \pmod 3$, we will refer to those members of the *hkl* family of reflections as the unbroadened subcomponents. Furthermore, those who satisfy $L_0 = \pm 1 \pmod 3$ will be referred to as the broadened subcomponents. Considering the broadened case, it is shown that the expression for the intensity in reciprocal space given by equation (1) becomes

$$I(h_1 h_2 h_3) = \psi^2 \sum_{m=-\infty}^{\infty} N_{|m|} \frac{3P_0(|m|) - 1}{2} \cos(2\pi |m| h_3/3), \quad (20)$$

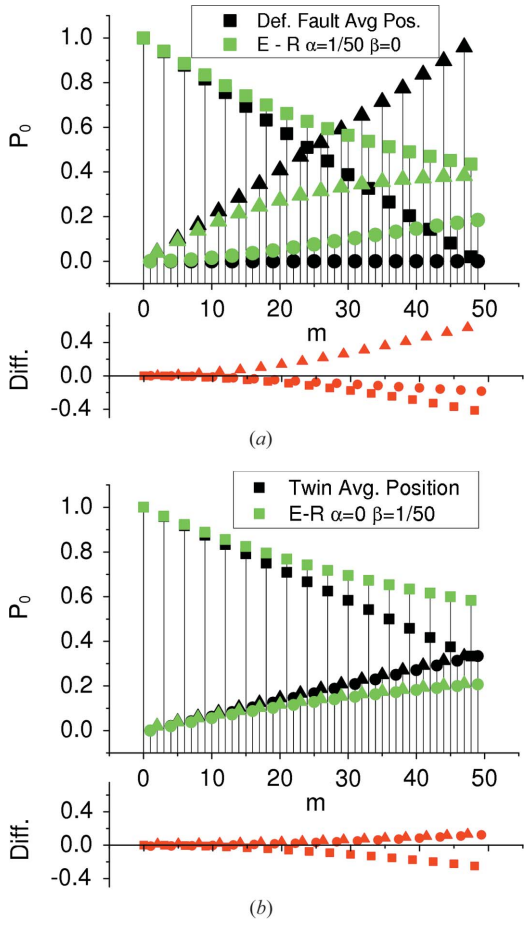

Figure 3
Comparison of $\overline{P_0(m)}$ with that given by the expression of E-R (Estevez-Rams *et al.*, 2008) for a stack of 50 planes containing (*a*) a deformation fault or (*b*) a twin fault. Below each figure the difference is given, Diff. $= (\overline{P_0(m)} - P_0^{\text{E-R}}(m))$. Again, the sets m_i are denoted by the same shapes as in Fig. 1.

as both $P_0(m)$ and N_m are mirrored about $m = 0$. The continuous variable h_3 can then be expressed in terms of its vicinity to the reciprocal-space point L_0,

$$h_3 = L_0 + \Delta h_3$$

After substituting this expression for h_3 into equation (20), expanding the cosine and properly accounting for the dependence of the sine function on $|m|$ into the amplitude coefficient, the sum in equation (20) becomes a Fourier series,

$$I(h_1 h_2 \Delta h_3) = \psi^2 \sum_{m=-\infty}^{\infty} A_m \cos(2\pi m \Delta h_3/3) + B_m \sin(2\pi m \Delta h_3/3), \tag{21a}$$

$$A_m = N_{|m|} \frac{3P_0(|m|) - 1}{2} \cos(2\pi m L_0/3) \text{ when } L_0 = \pm 1 \,(\text{mod } 3), \tag{21b}$$

$$B_m = -\frac{m}{|m|} N_{|m|} \frac{3P_0(|m|) - 1}{2} \sin(2\pi m L_0/3) \text{ when } L_0 = \pm 1 \,(\text{mod } 3). \tag{21c}$$

This expression then gives the general relation between the probability correlation function, $P_0(m)$, and the Fourier coefficients A_m and B_m. For the unbroadened subcomponents a similar Fourier series is found with coefficients of the form

$$A_m = N_{|m|} \text{ when } L_0 = 0 \,(\text{mod } 3)$$
$$B_m = 0 \text{ when } L_0 = 0 \,(\text{mod } 3),$$

which are not surprisingly only influenced by the stack size.

The powder-pattern intensity from a given *hkl* component can be approximated by remapping the intensity given in equation (21*a*) to that observed along the $\mathbf{s}_{hkl}$ direction (Velterop *et al.*, 2000; Warren, 1990), where $s_{hkl} = (h^2 + k^2 + l^2)^{1/2}/a = 2\sin\theta_{hkl}/\lambda$ and a is the f.c.c. unit-cell parameter. Therefore, the contribution to the peak profile from a single component of a family of reflections becomes

$$I(s_{hkl}, \Delta s) = \frac{I_e(\theta) N_a R \lambda^2 f^2(\theta) L(\theta) 3a^2 s_{hkl}}{16\pi V_a |L_0|} \times \sum_{m=-\infty}^{\infty} \left[\frac{A_m}{N} \cos\left(\frac{2\pi a^2 s_{hkl}}{L_0} m \Delta s \right) + \frac{B_m}{N} \sin\left(\frac{2\pi a^2 s_{hkl}}{L_0} m \Delta s \right) \right],$$

which is analogous to Warren's equation 13.59, and most of the variables have the same meaning. The only differences are that here N_a represents the number of atoms, V_a signifies the volume per atom, and $L(\theta)$ represents the Lorentz factor as the polarization factor is included in Warren's definition of $I_e(\theta)$ (see Warren, 1990, p. 29). Also, the term $1/B_3|\sin\varphi|$ used in Warren's expressions has been expressed here in the form $3a^2 s_{hkl}/L_0$.

The observed diffraction profile is then the sum of the peaks from all broadened and unbroadened subcomponents of an *hkl* reflection, and can be calculated following the considerations described by Velterop *et al.* (2000). To highlight the effect of faulting on the peak profile we will consider the intensity without contributions from the Lorentz polarization or atomic scattering factors defined as

$$I'(s_{hkl}, \Delta s) = \frac{3a^2 s_{hkl}}{|L_0|} \sum_{m=-\infty}^{\infty} \left[\frac{A_m}{N} \cos\left(\frac{2\pi a^2 s_{hkl}}{L_0} m \Delta s \right) + \frac{B_m}{N} \sin\left(\frac{2\pi a^2 s_{hkl}}{L_0} m \Delta s \right) \right]. \tag{22}$$

It should be noted that the peak broadening given by this formulation only considers the contributions from faulting and finite stack size normal to the fault plane. Peaks from small crystallites will also be broadened due to their small planar cross section. Therefore, the profiles presented here are not fully representative of the observable peaks from small crystallites containing faults, but are intended for the comparison of profile features that are the result of different faulting models.

As an example of how the powder diffraction peak is affected by different fault positions, a series of profiles of broadened subcomponents were calculated employing the probability correlation functions given by equations (7) and (13) for deformation and twin faults. The subcomponents broadened by deformation faults are depicted in Fig. 4 for a

series of fault positions in a stack of 50 Au (111) planes. It is seen that the profile shows the most broadening and shifting when the fault is in the center of the stack ($p = 25$) for all peaks considered. For this fault position, a large amount of asymmetry is observed in the peak shape, even to the extent that a second peak is apparent in the direction opposite to the peak shift. Moving the deformation fault closer to the boundary (decreasing p) has the effect of diminishing the features due to the deformation fault, and the contribution for size broadening becomes the defining characteristic. This behavior is best understood by considering that a fault has the most influence on $P_0(m)$ when it is at the stack center, as shown in Fig. 1. The more the correlation function deviates from that of a perfect stack, the more the peak profile is influenced.

The same study of the broadened components due to a twin fault at different positions is shown in Fig. 5. The effect of the twin on peak shape is different from that due to the deformation fault as the predominant effect is observed to be profile broadening. It is again found that the most broadened profile is obtained when the twin plane is in the center of the stack, and the broadening decreases as the fault moves toward the boundary.

In terms of the powder pattern the positional dependence is not as important as the average quantity. The diffraction profile due to a collection of crystallites which contain one fault and equal probability of all fault positions can also be calculated using equation (22), but now employing equations (15) and (16) to describe $P_0(m)$. Some resulting powder peaks, as well as the contributions from all subcomponents of the peak (broadened and unbroadened), are depicted in Fig. 6 for deformation faults, and Fig. 7 for twin faults. Also depicted in these figures are the profiles resulting from the E-R correlation functions, as well as the difference between the total profiles from the two models. In all cases the profiles are calculated assuming a stack of 50 Au (111) planes, with a faulting probability assumed to be 1/50.

The case of deformation faulting leads to the largest difference in peak profiles predicted by the two models. As shown in Fig. 6, the peaks from the developed average fault position model are more shifted and broadened than those found using the E-R model. The calculated 111 and 200 peaks are prime examples, as the calculated differences between the peak shapes are shown to reach as much as $\pm 20\%$ of the calculated intensities. For the patterns due to twinning a better agreement is found between the developed model and the E-R model. The peaks from the average position model show only slightly more broadening than the E-R model peaks. Again the 311 peaks are found to have the best agreement, as the 111 and 200 peaks differ by at most $\pm 10\%$ of the calculated intensities. Referring back to Fig. 3 it is apparent that the better agreement for the case of twinning stems from the fact that there is a better match between the two twin correlation functions than those for deformation faults.

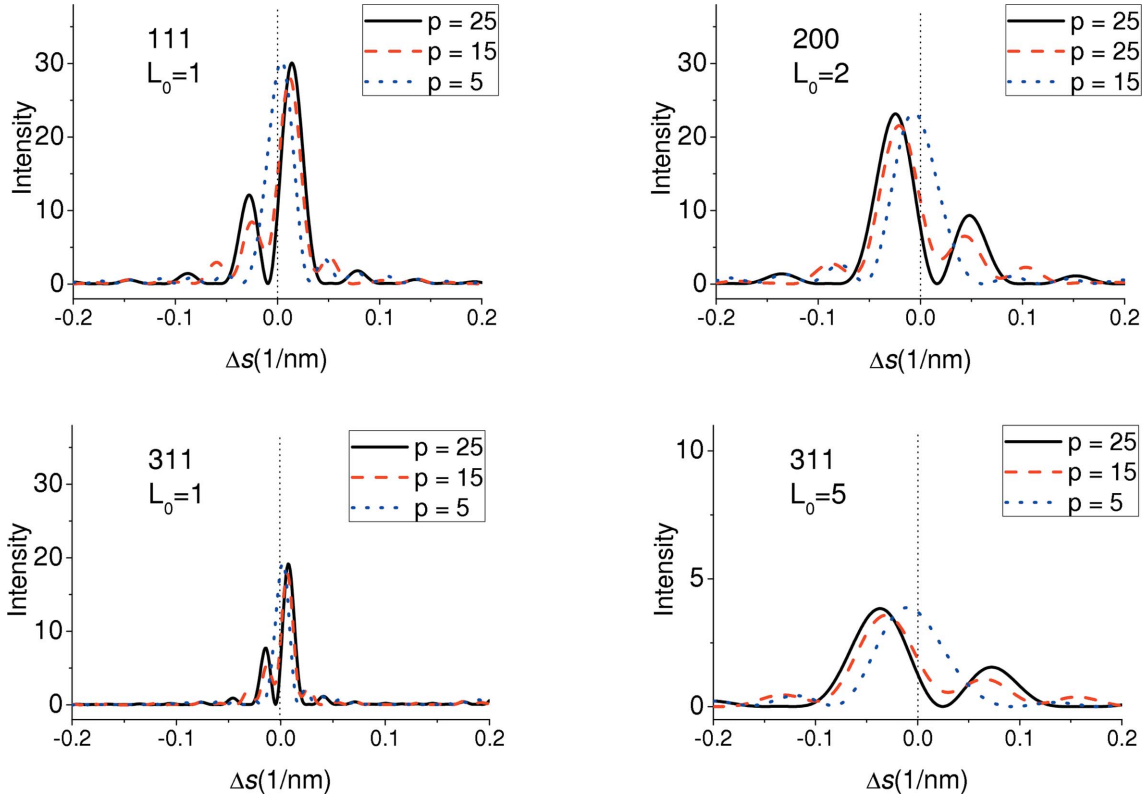

Figure 4
The extent of broadening and shifting caused by a deformation fault at different positions, p, is depicted for a few broadened subcomponents of powder diffraction peak profiles. A stack of 50 Au (111) planes with a lattice parameter a of 0.40809 nm was assumed in the calculation of the presented profiles. The case of $p = 25$ is then a fault at the center of the stack with the fault moving toward the left boundary as p is decreased.

7. Influence of $P_0(m)$ on peak broadening and asymmetry

To further study the influence of $P_0(m)$ on the broadened peak shape, the sum in equation (21*a*) can be rewritten as

$$\begin{aligned} I(h_1h_2\Delta h_3) = \psi^2 \sum_{n=-\infty}^{\infty} \big[& A_{3|n|-1}\cos(2\pi(3|n|-1)\Delta h_3/3) \\ & + B_{3|n|-1}\sin(2\pi(3|n|-1)\Delta h_3/3) \\ & + A_{3|n|}\cos(2\pi 3|n|\Delta h_3/3) \\ & + B_{3|n|}\sin(2\pi 3|n|\Delta h_3/3) \\ & + A_{3|n|+1}\cos(2\pi(3|n|+1)\Delta h_3/3) \\ & + B_{3|n|+1}\sin(2\pi(3|n|+1)\Delta h_3/3)\big]. \end{aligned}$$

After expanding the cosine and sine functions this is found to be equivalent to

$$I(h_1h_2h_3') = \psi^2 \sum_{n=-\infty}^{\infty} A_n'\cos(2\pi n\Delta h_3) + B_n'\sin(2\pi n\Delta h_3), \tag{23a}$$

$$\begin{aligned} A_n' = {} & A_{3|n|} + \cos(2\pi\Delta h_3/3)(A_{3|n|+1} + A_{3|n|-1}) \\ & + \sin(2\pi\Delta h_3/3)(B_{3|n|+1} - B_{3|n|-1}), \end{aligned} \tag{23b}$$

$$\begin{aligned} B_n' = {} & \frac{n}{|n|}\big[B_{3|n|} + \cos(2\pi\Delta h_3/3)(B_{3|n|+1} + B_{3|n|-1}) \\ & + \sin(2\pi\Delta h_3/3)(A_{3|n|-1} - A_{3|n|+1})\big]. \end{aligned} \tag{23c}$$

Substituting in equation (23) the expressions for A_m and B_m of equation (21) leads to the following relationships defining the coefficients of equation (23):

$$\begin{aligned} A_n' = {} & N_{3|n|}\Bigg[\cos(2\pi L_0/3)\frac{3P_0(3|n|)-1}{2} \\ & + \cos(2\pi(L_0+\Delta h_3)/3)\left(\frac{3(P_0(3|n|+1)+P_0(3|n|-1))}{2} - 1\right)\Bigg] \\ & + \frac{3(P_0(3|n|+1)-P_0(3|n|-1))}{2}, \end{aligned} \tag{24a}$$

$$\begin{aligned} B_n' = {} & -\frac{n}{|n|}\Bigg\{N_{3|n|}\Bigg[\sin(2\pi L_0/3)\frac{3P_0(3|n|)-1}{2} \\ & + \sin(2\pi(L_0+\Delta h_3)/3)\left(\frac{3(P_0(3|n|+1)-P_0(3|n|-1))}{2} - 1\right)\Bigg] \\ & + \frac{3(P_0(3|n|-1)-P_0(3|n|+1))}{2}\Bigg\}. \end{aligned} \tag{24b}$$

When n is small these coefficients are dominated by the part multiplied by $N_{3|n|}$. It is then evident in equation (24) that the cosine coefficients, A_n', which can be attributed to peak broadening, are largely dependent on the sum of the $P_0(m_1)$ and $P_0(m_2)$ terms. Furthermore, the sine coefficients, B_n', commonly attributed to peak asymmetry, are determined by the difference between these $P_0(m_1)$ and $P_0(m_2)$ terms. These relationships are true in general for any probability correla-

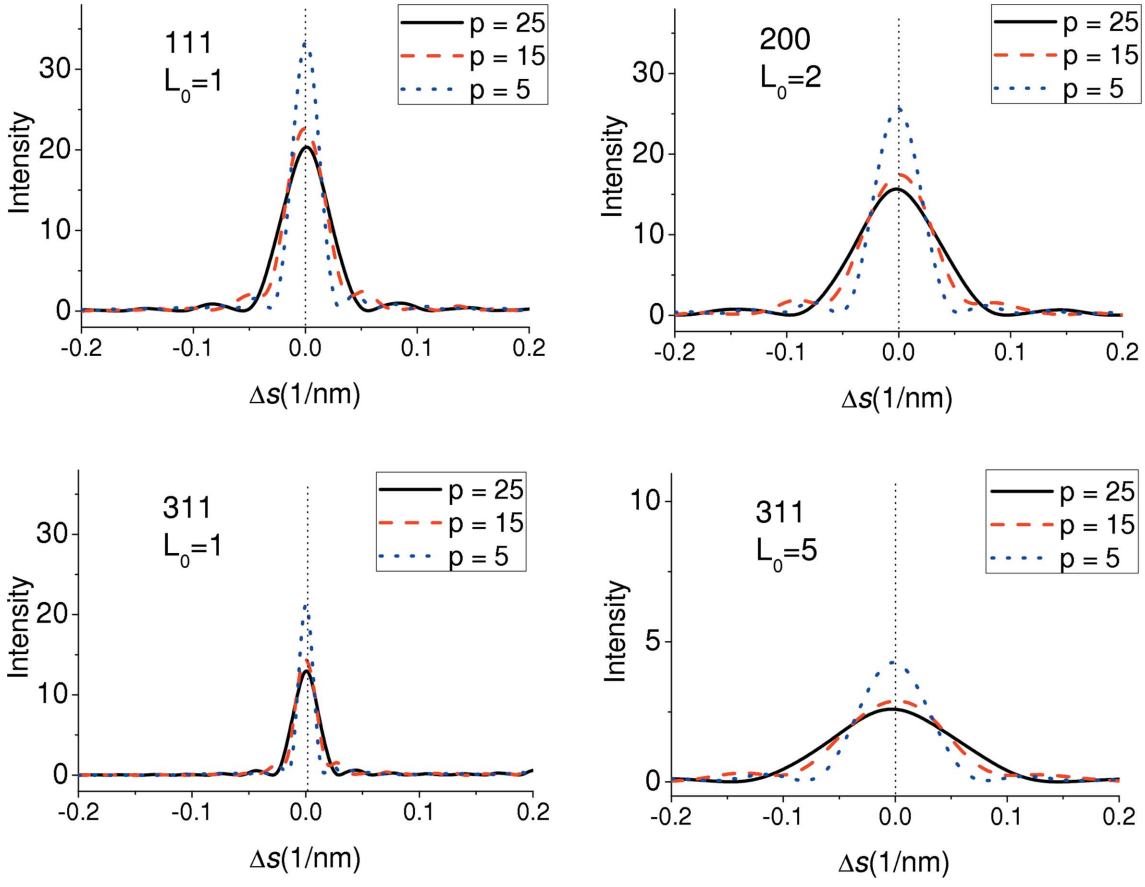

Figure 5
The extent of broadening caused by a twin fault at different positions, p, is depicted for a few broadened subcomponents of powder diffraction peak profiles. The assumptions of the size and type of stack used to calculate the profiles are the same as those given in Fig. 4.

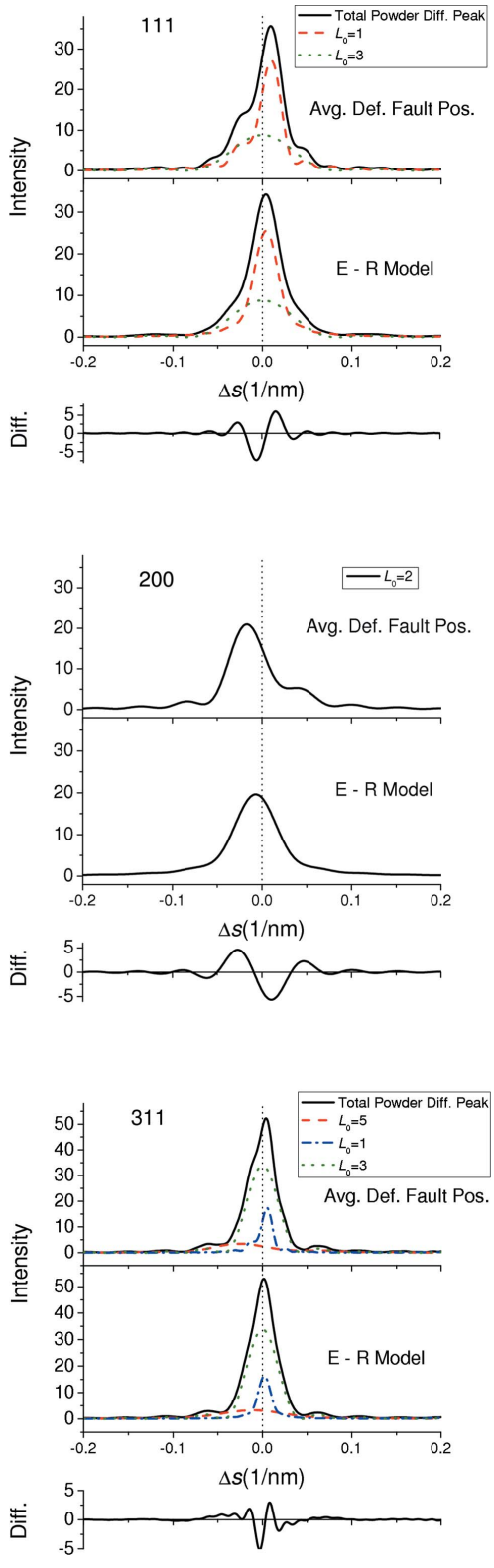

Figure 6
The subcomponents and total diffraction profiles are given for the 111, 200 and 311 peaks assuming both the average deformation fault position model, and the model for f.c.c. faulting developed by Estevez-Rams *et al.* (2008). For consistency the fault probabilities assumed in the E-R model were $\alpha = 1/50$ and $\beta = 0$. Below the calculated peaks is the difference between the total profiles given from the relation, Diff. $= I_{\text{Avg.Pos.}} - I_{\text{E-R}}$. In each peak the 'broadened' components are depicted by dashed lines, while the 'unbroadened' component is depicted by a dotted line.

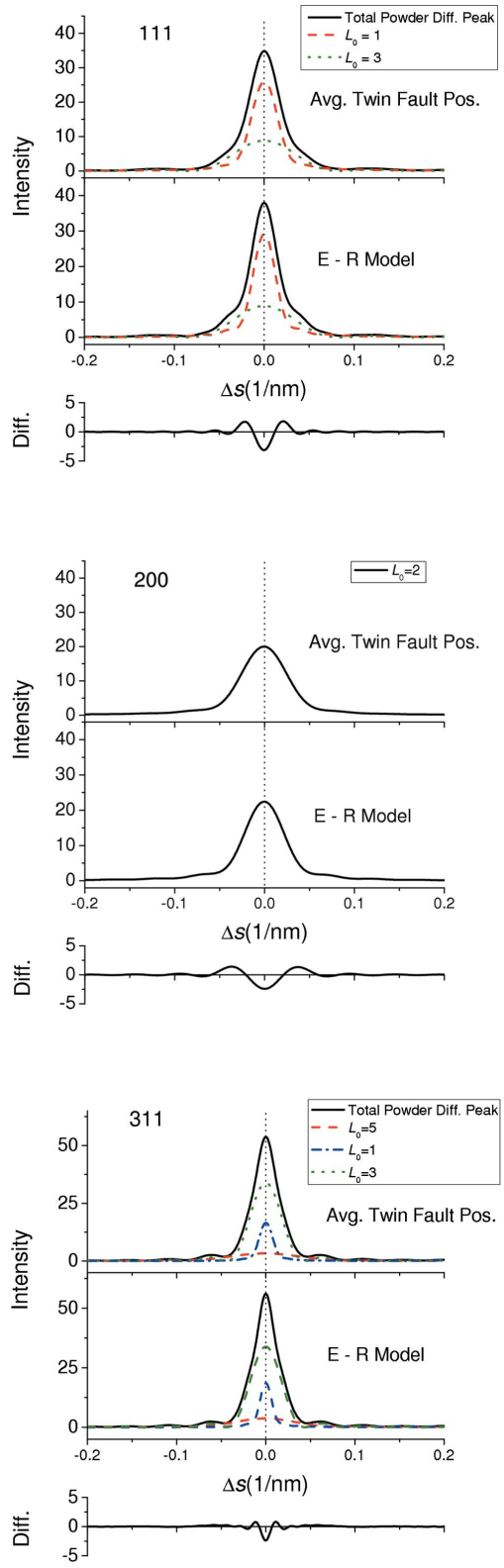

Figure 7
The subcomponents and total diffraction profiles are given for the 111, 200 and 311 peaks assuming the average twin-fault position model, and the model for f.c.c. faulting developed by Estevez-Rams *et al.* (2008). In this case the fault probabilities assumed in the E-R model were $\alpha = 0$ and $\beta = 1/50$. The difference between models and the components of each peak are depicted in the same way as described in Fig. 6.

tion function of an f.c.c. stacking. In terms of our study this is the key to explaining why the peak shape of a stack containing a deformation fault exhibits an asymmetry and shift, whereas that containing a twin is primarily broadened. The correlation function derived for a deformation fault in equation (15) has a difference in the $P_0(m_1)$ and $P_0(m_2)$ terms given by $-P_0(m_2)$, whereas this difference for a twin fault, from equation (16), is nearly zero except when there are few planes in the stacking.

It can then be argued that some of the observed shift in peak position commonly attributed to deformation faults is actually a consequence of the *strong* peak asymmetry. This result maybe somewhat surprising since, following the treatment of Warren (1990), it is commonly believed that any peak asymmetry is only due to twin faulting. As shown in Fig. 7, it is not incorrect that peaks broadened by twins exhibit slight asymmetry, however, the fact that the profiles from deformation faults also result in peak asymmetry calls into question the validity of methods which rely solely on the peak asymmetry and peak shift to quantify the deformation and twin fault densities.

The true limit of information obtainable from studying a faulted f.c.c. powder diffraction peak profile is found by considering that due to the nature of the Fourier series, such as that in equation (24), a profile can only be uniquely linked to an average $P_0(m)$. Therefore, if multiple faulting scenarios result in the same average correlation function, then powder diffraction cannot distinguish between them. The separation of the faulting effect from the broadening due to crystallite size and other strains is only possible by simultaneously considering the profiles of multiple reflections in the pattern. The modified Williamson–Hall analysis is one proposed method to consider the effect of faulting on the broadening of multiple reflections (Ungár *et al.*, 1998). However, only information on the peak in terms of its full-width half-maximum (FWHM) or integral breadth (IB) is used to determine the faulting densities. In the process of simplifying the treatment, important information about the complicated shape of the peak from the many subcomponents and faulting effects is neglected (Velterop *et al.*, 2000), making the fault densities found from this method quantitatively less reliable (Scardi *et al.*, 2004). A slightly more sophisticated treatment has recently been proposed in the convolutional multiple whole profile (CMWP) modeling framework, which has parametrized the influence of different fault probabilities on the FWHM, asymmetry and peak positions of profile subcomponents (Balogh *et al.*, 2006). While accounting for some aspect of the peak shape by considering multiple subcomponents, the description of the profiles in terms of a few parameters again neglects a fair amount of information in the peak shape and use of a Lorentzian function to describe the peak shape may bias the results. Just by inspecting the subcomponents of peak profiles simulated in the present paper it is quickly concluded that a profile due to faulting is not necessarily Lorentzian, or any other analytical peak function, but is instead determined from the probability correlation function. Given the complexity of determining a reasonable faulting density from the powder pattern it is best to utilize all the information possible from the measured intensity, and properly treat the peak as the Fourier transform of a real physical model. These are the fundamental assumptions of the whole powder pattern modeling (WPPM) method, which has been developed to consider the most recent models of faulting in f.c.c. materials (Estevez-Rams *et al.*, 2008; Scardi & Leoni, 2002).

8. Discussion

The fundamental differences between the disorder caused by a deformation fault *versus* a twin fault has been clearly traced, through the probability correlation function, to their effects on the diffraction peak profile. Furthermore, when considering a finite stack the planar correlations have been shown not only to depend on the fault position, but also on the extent of the stack when considering twin faults, implying the same must be true for the diffraction profile. In fact, recent simulation studies have found that the presence of a fault at different positions in a spherical nanocrystallite results in similar trends on the peak broadening and shifting, as well as dramatic differences in the observed fault probability (Beyerlein *et al.*, 2011). This is evidence that the description of broadening which has been presented is not completely masked by the broadening due to the small cross section of a nanocrystallite. Nonetheless, for a proper description of the peak profile from such a case, a convolution of the described features in the intensity with those due to the particle size and shape must be made. As the general form of the Fourier coefficients is given in equation (21), modern reciprocal-space modeling techniques like WPPM (Scardi & Leoni, 2002) show promise in utilizing the developed model and performing this convolution in reciprocal space. The same can be said regarding the use of the developed model to describe the effect of faulting in powders of crystallites with a broad size distribution. The development of such a robust line-profile analysis tool is ongoing, along with experimental validation of the proposed model to describe faulting in small crystallites.

When considering the average correlation function, the model allows for considerable flexibility as the possibilities for different average planar correlation functions extend far beyond the uniform fault position distribution demonstrated in §4. If a more complex fault position distribution is found to be suitable for a given system, then only the weights, w_p, in equation (14) need to be adjusted and the resulting peak profile recalculated.

The current limiting assumption of the developed model is that only one fault is allowed to exist in a given crystallite. In this regard it might be true that the recursion equation model (Warren, 1990; Estevez-Rams *et al.*, 2008) is more appropriate to represent faulting in many f.c.c. materials, especially those with a large crystallite size. Accounting for multiple faults in the developed theoretical framework is not impossible, but becomes increasingly complex as the number of cases to consider increases with the number of faults. For example, a finite stack containing just two faults requires the consideration of each fault being either a deformation fault or twin

fault, as well as all the different possible distances between faults and their positions relative to the boundaries. With the computation power available in modern desktop computers, it might be better suited to directly compute the correlation functions and averages of the desired faulting scenarios. In which case, the general expression of equation (21) is still applicable to model the peak profile from the calculated correlation functions.

References

Balogh, L., Ribárik, G. & Ungár, T. (2006). *J. Appl. Phys.* **100**, 023512.
Beyerlein, K. R., Leoni, M., Snyder, R. L. & Scardi, P. (2011). *Mater. Sci. Forum*, **681**, 13–18.
Cervellino, A., Giannini, C. & Guagliardi, A. (2003). *J. Appl. Cryst.* **36**, 1148–1158.
Estevez-Rams, E., Penton Madrigal, A., Scardi, P. & Leoni, M. (2007). *Z. Kristallogr.* Suppl. **26**, 99–104.
Estevez-Rams, E., Welzel, U., Pentón Madrigal, A. & Mittemeijer, E. J. (2008). *Acta Cryst.* A**64**, 537–548.
Hendricks, S. & Teller, E. (1942). *J. Chem. Phys.* **10**, 147–167.
Hendricks, S. B., Jefferson, M. E. & Shultz, J. F. (1930). *Z. Kristallogr.* **73**, 376–380.
Jagodzinski, H. (1949*a*). *Acta Cryst.* **2**, 201–207.
Jagodzinski, H. (1949*b*). *Acta Cryst.* **2**, 208–214.
Marks, L. D. (1994). *Rep. Prog. Phys.* **57**, 603–649.
Scardi, P. & Leoni, M. (2002). *Acta Cryst.* A**58**, 190–200.
Scardi, P., Leoni, M. & Delhez, R. (2004). *J. Appl. Cryst.* **37**, 381–390.
Treacy, M. M. J., Newsam, J. M. & Deem, M. W. (1991). *Proc. R. Soc. London Ser. A*, **43**, 499–520.
Ungár, T., Ott, S., Sanders, P. G., Borbély, A. & Weertman, J. R. (1998). *Acta Mater.* **46**, 3693–3699.
Velterop, L., Delhez, R., de Keijser, Th. H., Mittemeijer, E. J. & Reefman, D. (2000). *J. Appl. Cryst.* **33**, 296–306.
Warren, B. E. (1990). *X-ray Diffraction*, pp. 275–288. New York: Dover.
Wilson, A. J. C. (1942). *Proc. R. Soc. London Ser. A*, **180**, 277–285.